COMPARING M31 AND MILKY WAY SATELLITES: THE EXTENDED STAR FORMATION HISTORIES OF ANDROMEDA II AND ANDROMEDA XVI[*]

Daniel R. Weisz[1,2,19], Evan D. Skillman[3], Sebastian L. Hidalgo[4,5], Matteo Monelli[4,5], Andrew E. Dolphin[6], Alan McConnachie[7], Edouard J. Bernard[8], Carme Gallart[4,5], Antonio Aparicio[4,5], Michael Boylan-Kolchin[9], Santi Cassisi[10], Andrew A. Cole[11], Henry C. Ferguson[12], Mike Irwin[13], Nicolas F. Martin[14,15], Lucio Mayer[16,17], Kristen B. W. McQuinn[3], Julio F. Navarro[18], and Peter B. Stetson[7]

[1] Department of Astronomy, University of California at Santa Cruz, 1156 High Street, Santa Cruz, CA 95064, USA; drw@ucsc.edu
[2] Astronomy Department, Box 351580, University of Washington, Seattle, WA, USA
[3] Minnesota Institute for Astrophysics, University of Minnesota, Minneapolis, MN, USA
[4] Instituto de Astrofísica de Canarias. Vía Láctea s/n., E-38200 La Laguna, Tenerife, Canary Islands, Spain
[5] Department of Astrophysics, University of La Laguna. Vía Láctea s/n., E-38200 La Laguna, Tenerife, Canary Islands, Spain
[6] Raytheon, 1151 E. Hermans Road, Tucson, AZ 85706, USA
[7] Dominion Astrophysical Observatory, Herzberg Institute of Astrophysics, National Research Council,
5071 West Saanich Road, Victoria, BC V9E 2E7, Canada
[8] Institute for Astronomy, University of Edinburgh, Royal Observatory, Blackford Hill, Edinburgh EH9 3HJ, UK
[9] Astronomy Department, University of Maryland, College Park, MD, USA
[10] INAF-Osservatorio Astronomico di Collurania, Teramo, Italy
[11] School of Mathematics & Physics, University of Tasmania, Hobart, Tasmania, Australia
[12] Space Telescope Science Institute, 3700 San Martin Drive, Baltimore, MD 21218, USA
[13] Institute of Astronomy, University of Cambridge, Madingley Road, Cambridge CB3 0HA, UK
[14] Observatoire astronomique de Strasbourg, Universit de Strasbourg, CNRS,
UMR 7550, 11 rue de l'Universit, F-67000 Strasbourg, France
[15] Max-Planck-Institut fr Astronomie, Knigstuhl 17, D-69117 Heidelberg, Germany
[16] Institut für Theoretische Physik, University of Zurich, Zürich, Switzerland
[17] Department of Physics, Institut für Astronomie, ETH Zürich, Zürich, Switzerland
[18] Department of Physics and Astronomy, University of Victoria, BC V8P 5C2, Canada

ABSTRACT

We present the first comparison between the lifetime star formation histories (SFHs) of M31 and Milky Way (MW) satellites. Using the Advanced Camera for Surveys on board the *Hubble Space Telescope*, we obtained deep optical imaging of Andromeda II (And II; $M_V = -12.0$; $\log(M_\star/M_\odot) \sim 6.7$) and Andromeda XVI (And XVI; $M_V = -7.5$; $\log(M_\star/M_\odot) \sim 4.9$) yielding color–magnitude diagrams that extend at least 1 mag below the oldest main-sequence turnoff, and are similar in quality to those available for the MW companions. And II and And XVI show strikingly similar SFHs: both formed 50%–70% of their total stellar mass between 12.5 and 5 Gyr ago ($z \sim 5$–0.5) and both were abruptly quenched $\sim$5 Gyr ago ($z \sim 0.5$). The predominance of intermediate age populations in And XVI makes it qualitatively different from faint companions of the MW and clearly not a pre-reionization fossil. Neither And II nor And XVI appears to have a clear analog among MW companions, and the degree of similarity in the SFHs of And II and And XVI is not seen among comparably faint-luminous pairs of MW satellites. These findings provide hints that satellite galaxy evolution may vary substantially among hosts of similar stellar mass. Although comparably deep observations of more M31 satellites are needed to further explore this hypothesis, our results underline the need for caution when interpreting satellite galaxies of an individual system in a broader cosmological context.

Key words: galaxies: dwarf – galaxies: individual (And II, And XVI) – Galaxy: evolution – Galaxy: formation – Local Group

Online-only material: color figures

1. INTRODUCTION

Our current understanding of satellite and low-mass galaxy evolution primarily comes from the Milky Way (MW) companions. Their close proximities ($D \lesssim 300$ kpc) enable a variety of detailed measurements including stellar abundances, radial and tangential velocities, stellar velocity dispersions, and deep resolved star color–magnitude diagrams (CMDs), which provide complementary constraints on their star formation and dynamical histories (e.g., Gallart et al. 2005; Tolstoy et al. 2009; Kirby et al. 2011; Brown et al. 2012; Sohn et al. 2013; Weisz et al. 2014). Due to the availability of such detailed measurements, the MW companions are often used either explicitly or implicitly as the observable benchmarks for cosmological simulations of low-mass galaxies and satellites systems (e.g., Muñoz et al. 2009; Busha et al. 2010; Rocha et al. 2012; Assmann et al. 2013; Kazantzidis et al. 2013; Starkenburg et al. 2013). Considering their unique role as population templates, it is vitally important that we understand whether they are representative of satellites in the broader universe.

Testing the representative nature of the MW satellites requires comparison with other satellite populations. While deep imaging

Table 1
Observational Properties of Andromeda II and Andromeda XVI

Quantity	And II	And XVI
(1) R.A. (J2000)	01:16:27.0	00:59:29.8
(2) Decl. (J2000)	$+33$:26:05.6	$+32$:22:31.4
(3) $(m-M)_0$	24.07 ± 0.06	23.60 ± 0.2
(4) M_V	-12.0 ± 0.1	-7.5 ± 0.3
(5) A_V	0.17	0.18
(6) r_h (′)	5.1 ± 0.1	$0.93^{+0.16}_{-0.09}$
(7) Obs. dates	2013 Oct 4–6	2013 Nov 20–22
(8) Orbits	17	13
(9) Exp. time (F475W, F814W) (s)	22472, 17796	17194, 13622
(10) 50% completeness (F475W, F814W)	28.8, 27.9	28.8, 27.8
(11) Stars in CMD	80164	7695

Notes. Basic observational properties of And II and And XVI. (1)–(3) are from McConnachie (2012), (4) and (6) are from N. F. Martin (in preparation), (5) is from Schlafly & Finkbeiner (2011).

of the MW satellites is possible with ground-based telescopes (e.g., Sand et al. 2010; Okamoto et al. 2012; del Pino et al. 2013) most other systems are too distant for obtaining comparably detailed observations, making direct comparisons with the MW companions impossible. The exception is the M31 group. Its diversity of satellites and close proximity ($D \sim 780$ kpc; Conn et al. 2012) allow for observations that approach the level of detail available in the MW companions, making it an excellent foil to the MW.

Currently, there is tentative evidence for systematic differences between the M31 and MW satellites. Several studies suggest that the M31 satellites follow a different size–mass relationship than the MW companions (e.g., McConnachie & Irwin 2006; Kalirai et al. 2010; although, see Brasseur et al. 2011; Tollerud et al. 2012 for an alternative interpretation) that may be related to systematically different dark matter profiles and/or a complex history of tidal interactions (e.g., Mayer et al. 2001; Collins et al. 2014). The sub-groups also differ in their large-scale structural properties. M31 hosts a rich set of streams, orphaned globular clusters, and a thin corotating plane of satellites (e.g., McConnachie et al. 2009; Huxor et al. 2011; Ibata et al. 2013; Martin et al. 2013). In contrast, the MW sub-group appears to have fewer stream-like structures, orphan clusters, and a polar-oriented satellite configuration (e.g., Lynden-Bell 1976; Belokurov et al. 2006; Pawlowski et al. 2012). These structural differences are believed to trace the contrasting accretion histories of the two sub-groups (e.g., Shaya & Tully 2013).

Despite tantalizing differences in the present-day satellite properties, little is known about the relative temporal evolution of the M31 and MW satellites. While the MW companions have ubiquitously deep CMDs and well-constrained star formation histories (SFHs; $\lesssim 1$ Gyr resolution at all ages; e.g., Tolstoy et al. 2009; Weisz et al. 2014), no comparable measurements have been made in the M31 group. Existing ground- and space-based imaging of the M31 satellites have only resulted in CMDs that include the horizontal branch (HB), which are excellent for distance determinations, identifying new galaxies and clusters, and coarse stellar population characterization (e.g., Da Costa et al. 1996, 2000, 2002; McConnachie & Irwin 2006; Yang & Sarajedini 2012), but are not suitably deep for well-constrained SFH measurements at all epochs (e.g., Gallart et al. 2005; Weisz et al. 2014). As a result, we have little knowledge of major milestones in the M31 satellites histories such as the timing of the first epoch of star formation, the temporal patterns of

stellar mass assembly, and the epochs of quenching, all crucial questions that have been answered for the MW companions through analysis of SFHs derived from deep CMDs (Tolstoy et al. 2009; Weisz et al. 2014 and references therein).

In this paper, we undertake the first direct comparison of the lifetime SFHs of M31 and MW satellites. Using observations taken with the Advanced Camera for Surveys (ACS; Ford et al. 1998) on board the *Hubble Space Telescope* (*HST*), we have measured the SFHs of two M31 companions, Andromeda II (And II) and Andromeda XVI (And XVI), from CMDs that extend below the oldest main-sequence turnoff (MSTO). The exceptional depth of these CMDs ensures that the resulting SFHs are directly comparable to the SFHs of MW companions, providing a first look at the temporal evolution of two satellite populations.

This paper is organized as follows. We describe the observations, photometric reductions, and CMDs in Section 2 and outline the SFH measurement method in Section 3. In Section 4, we present the SFHs of And II and And XVI, compare them with MW companion SFHs in Section 5. We summarize our results in Section 6. Throughout this paper, the conversion between age and redshift assumes the Planck cosmology as detailed in Planck Collaboration (2013).

2. THE DATA

2.1. Observations and Photometry

Our observational and data reduction strategy follows that of our previous program: Local Cosmology with Isolated Dwarfs (LCID). Here, we briefly summarize that strategy and refer the reader to Monelli et al. (2010) for more details.

We obtained a single central field of *HST*/ACS imaging in both And II and And XVI between 2013 October 4 and 6 and 2013 November 20 and 22, respectively. In each galaxy, we also acquired an outer parallel field with the Wide Field Camera 3 (WFC3; Kimble et al. 2008). In this paper, we focus on results from the central ACS fields, and will address the spatial dependences of the stellar populations in future papers. Basic properties of both galaxies are listed in Table 1.

We observed both galaxies in the F475W (Sloan *g*) and F814W (*I*). The observations were taken over multiple orbits with a four step dither pattern in order to reject hot pixels and cosmic rays. The images were taken with a cadence that optimized the observations of short-period variable stars, which will also be presented in future papers.

We performed point-spread function (PSF) photometry on the newly released charge transfer efficiency corrected images (i.e., `flc` images) for both galaxies using DOLPHOT, an updated version of HSTPHOT with an ACS specific module (Dolphin 2000). Following the LCID strategy, we also performed photometry with DAOPHOT/ALLFRAME (Stetson 1994), and found no significant differences between the resulting CMDs, which is identical to the conclusions of the extensive photometric testing presented in Monelli et al. (2010) and Hidalgo et al. (2011). The remainder of this paper uses the DOLPHOT photometry.

From the raw photometric catalog, we rejected objects that did not meet particular requirements in signal-to-noise (S/N), PSF profile sharpness, and whose flux was significantly affected by neighboring objects. Specifically, our accepted stars have $\mathrm{S/N}_{F475W}$ and $\mathrm{S/N}_{F814W} > 5$, $(\mathrm{sharp}_{F475W} + \mathrm{sharp}_{F814W})^2 < 0.1$, and $(\mathrm{crowd}_{F475W} + \mathrm{crowd}_{F814W}) < 1.0$. The precise definitions of these criteria can be found in Dolphin (2000).

To characterize the completeness and observational uncertainties, we inserted $\gtrsim 5 \times 10^5$ artificial stars in the observed
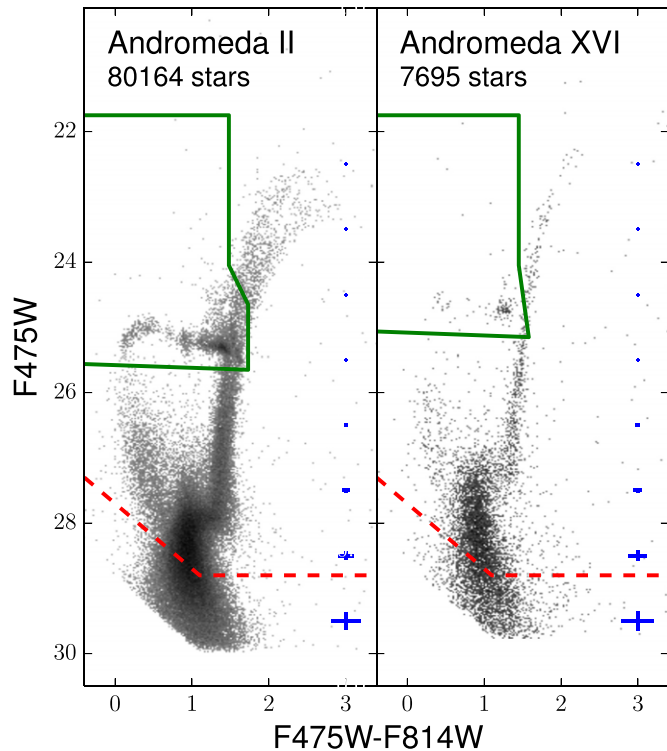
Figure 1. *HST*/ACS-based CMDs for And II and And XVI. To enhance visibility of key CMD features over a large dynamic range of stellar densities, we plotted these as Hess diagrams, i.e., finely binned CMDs. The red-dashed lines reflect the 50% completeness limits. We excluded less certain phases of stellar evolution such as the horizontal branch and red clump from the CMDs fits, as indicated by the green polygons.

(A color version of this figure is available in the online journal.)

images and recovered their photometry in an identical manner to the real photometry.

2.2. Color–Magnitude Diagrams

In Figure 1, we have plotted the CMDs of And II and And XVI. In both systems, the photometry is 50% complete to ∼1 mag below the oldest MSTO, providing for excellent leverage on the ancient SFHs of both systems. The observations for both galaxies are several magnitudes deeper than any previous ground- or *HST*-based photometry of M31 satellites, making them the deepest observations ever obtained of satellite galaxies outside the virial radius of the MW.

The two CMDs show several interesting features. Most notably, And II shows a split red giant branch (RGB), which indicates the presence of distinct age and/or metallicity populations. It is the only known dwarf galaxy with a distinct double RGB. Additionally, the CMD of And II exhibits an extended red clump (RC), well-populated blue and red HBs, and a sub-giant branch (SGB) that is broad in luminosity.

The CMD of And XVI displays fewer distinct features and has lower stellar density, relative to And II. However, it too shows both a blue and red HB and an SGB that spans a brand range in luminosity, both of which may be indicative of an extended SFH. We discuss the detailed SFHs of both galaxies in Section 4.

3. MEASURING THE STAR FORMATION HISTORY

We have measured the SFHs of both galaxies using the CMD fitting package MATCH (Dolphin 2002). Briefly, MATCH constructs a set of synthetic simple stellar populations (SSPs) based on

user defined parameters such as a stellar initial mass function, age and metallicity bins, and searchable ranges in distance and extinction. The synthetic SSPs are linearly combined and added to a model foreground population (from the empirical model in de Jong et al. 2010) to form a composite synthetic CMD, which is then convolved with observational biases from artificial star tests. MATCH compares the model and observed CMDs using a Poisson likelihood statistic. The SFH that corresponds to the best-matched synthetic CMD is the most likely SFH of the observed population. A full description of MATCH can be found in Dolphin (2002). The fitting of these CMDs uses the Padova stellar models (Girardi et al. 2002, 2010) and follows the fitting methodology from Weisz et al. (2014), with one exception: instead of fitting the full CMD, we excluded the RC and HB from the fit in order to mitigate the contribution of these relatively less certain phases of stellar evolution to the SFH (Aparicio & Hidalgo 2009). Throughout this paper, the plotted uncertainties reflect the 68% confidence interval around the best-fit SFH due to both random uncertainties (from a finite number of stars on the CMD) and systematic uncertainties (due to uncertain physics in the underlying stellar models). We refer the reader to Dolphin (2012) for a full discussion of systematic uncertainties and Dolphin (2013) for a detailed description of random uncertainties in SFH measurements.

Following the LCID strategy, we tested the robustness of our SFHs by analyzing the data with a second CMD fitting package and a different set of stellar libraries. In this case, we used IAC-POP (Aparicio & Hidalgo 2009) and the BaSTI stellar libraries (Pietrinferni et al. 2004) to measure the SFHs of both data sets. Significant testing of the effects of excluding different parts of the CMD were also conducted (cf. Monelli et al. 2010). Overall, we found the solutions to be consistent within the plotted uncertainties and for the purpose of this paper, we will not discuss the details of these comparisons further and will use the MATCH-based SFHs.

4. THE STAR FORMATION HISTORIES OF AND II AND AND XVI

In this paper, we focus on the cumulative SFHs, i.e., the fraction of stellar mass formed prior to a given epoch, which allow us to readily compare multiple SFHs on the same normalized scale, and are presented in Figure 2. For reference, the age–metallicity relationships (AMRs) for both galaxies are plotted in Figure 3. We will undertake a detailed interpretation of the AMRs and the absolute SFHs in future papers.

We first consider the SFH of And II. As shown in the top panel of Figure 2, And II formed ∼50% of its total stellar mass prior to ∼12.5 Gyr ago ($z \sim 5$) and ∼50% of its stellar mass from 12.5–5 Gyr ago ($z \sim 5$–0.5). The initial burst was followed by a slower rate of mass growth from ∼12.5–10 Gyr ago ($z \sim 5$–2), and an enhanced interval of star formation from ∼10–5 Gyr ago ($z \sim 2$–0.5). Our findings indicate that And II had two distinct elevated periods of star formation, which will be discussed in detail in future papers. Star formation in And II was quenched at ∼5 Gyr ago ($z \sim 0.5$).

Is it interesting to consider the SFH of And II in light of its unusual properties. From Subaru imaging, McConnachie et al. (2007) first noted that And II has two distinct stellar populations: one centrally concentrated, metal-rich population and another extended, metal-poor population, similar to MW dwarfs such as Sculptor and Fornax (e.g., Tolstoy et al. 2004). However, And II hosts a more spatially extended light profile than either Sculptor or Fornax (e.g., McConnachie et al. 2007). Recently, And II
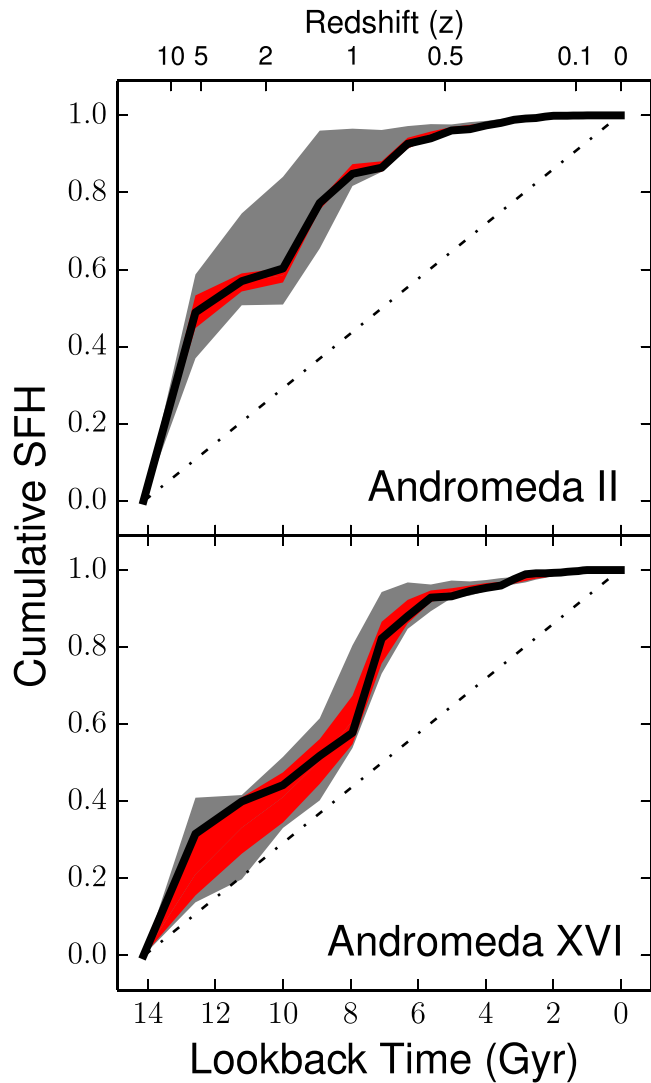
Figure 2. Cumulative SFHs, i.e, the fraction of total stellar mass formed prior to a given epoch, of And II and And XVI. The dot-dashed line reflects a constant lifetime star formation rate. Random uncertainties are highlighted in color and the total uncertainties (random plus systematic) are shown in gray. The larger uncertainties for And XVI are due to the smaller number of observed stars.

(A color version of this figure is available in the online journal.)
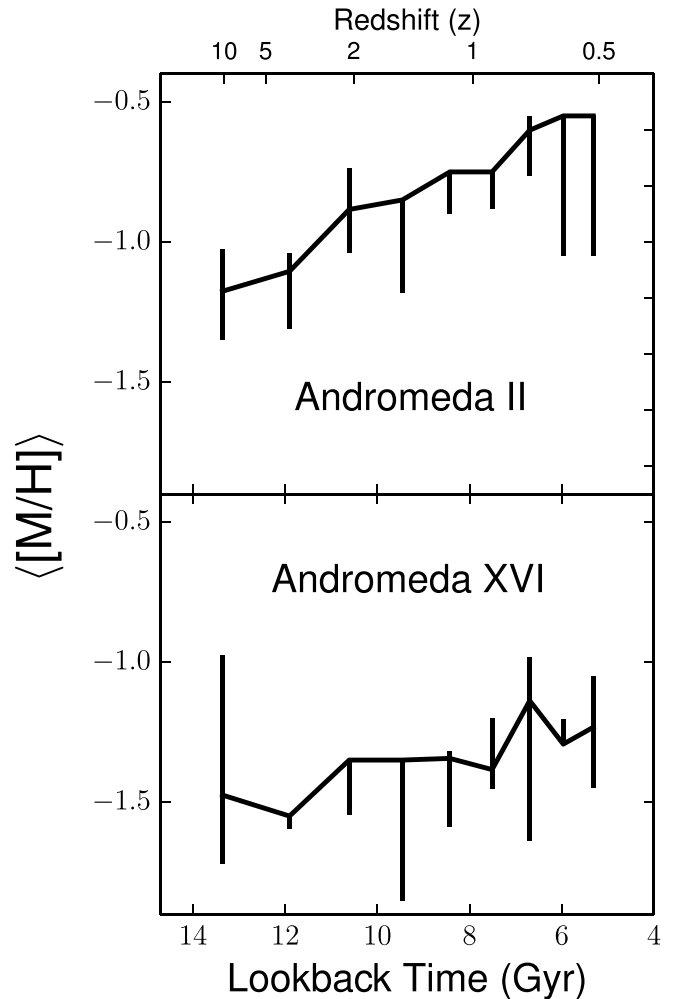

Figure 3. Age–metallicity relationships of And II and And XVI over their intervals of active star formation. The solid lines reflect the mean metallicity, and the error bars are the total uncertainties, i.e., random and systematic.

has been shown to both rotate about its minor axis (Ho et al. 2012) and host a kinematically cold stellar stream (Amorisco et al. 2014), both of which are unique features among low-mass galaxies. Unfortunately, our CMD is entirely contained inside the stellar stream, making it challenging to directly tie our SFH to the merger scenario proposed by Amorisco et al. (2014). In a future paper, we will leverage the wide-field ground based imaging along with our ACS and WFC3 observations to explore spatial variations in the populations of And II, which may provide new insight into its unusual history.

The SFH of And XVI, shown in the bottom panel of Figure 2 is similar to And II, and hosts a mix of ancient and intermediate age populations. And XVI formed ~30% of its stellar mass prior to 12.5 Gyr ago ($z \sim 5$) and 70% of its mass between 12.5 and 5 Gyr ago ($z \sim 5$–0.5). Star formation in And XVI was also quenched at ~5 Gyr ago ($z \sim 0.5$).

The extended SFH of And XVI is particularly intriguing in the context of cosmic reionization. Several theoretical models predict that extremely low-mass galaxies ($M_\star \lesssim 10^6 \, M_\odot$) should

have had their star formation quenched ~12.8–13.5 Gyr ago ($z \sim 6$–14) due to heating of its gas by ultraviolet radiation from cosmic reionization (so-called "fossils of reionization"; e.g., Ricotti & Gnedin 2005). Based on its low stellar mass ($M_\star \sim 10^5 \, M_\odot$) and large distance from M31 ($D \sim 280$ kpc), which reduces the role of environmental influence from M31, And XVI is an ideal fossil candidate. However, its large intermediate age population and continuous SFH strongly rule out reionization as a quenching mechanism.

Despite being nearly two orders of magnitude apart in stellar mass, And II and And XVI have extended SFHs that track one another remarkably well, as illustrated in Figure 4. Following the initial epoch of star formation, both galaxies show declines in stellar mass growth beginning ~12.5 Gyr ago, followed by brief increases in star formation activity, before finally being quenched at similar epochs of ~5 Gyr ago ($z \sim 0.5$). While our small sample size cannot rule out chance coincidence, there are also speculative physical explanations for the similarity of their SFHs. One possibility is that both galaxies may have similar halo masses, enabling them to retain gas for similar timescales. The difference in stellar mass could potentially be attributed to large scatter in stellar mass at a fixed halo mass as discussed in Boylan-Kolchin et al. (2011) and Garrison-Kimmel et al. (2014). Another possibility is that both galaxies closely passed by M31 at similar times, but had different orbital trajectories
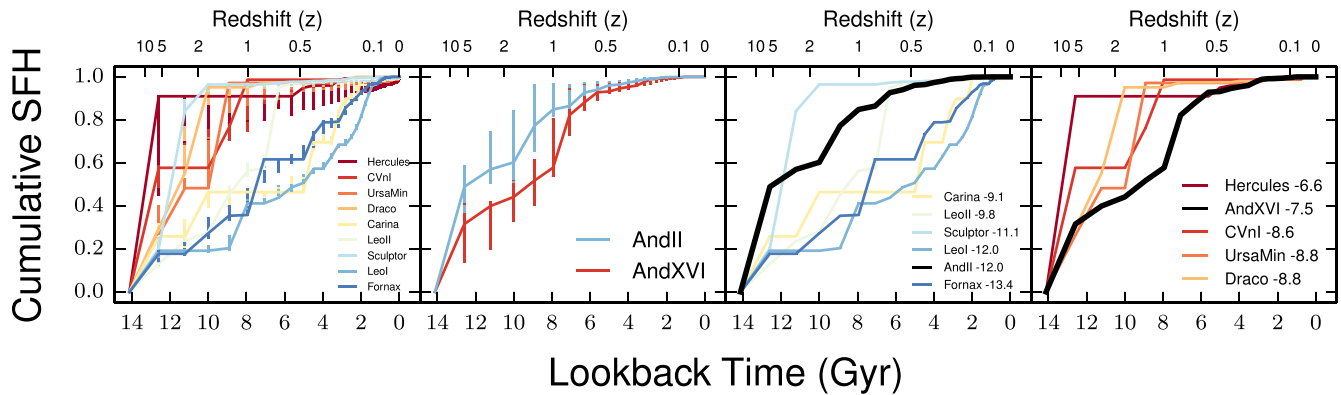
Figure 4. Comparison between the SFHs of MW and M31 companions. Left: the SFHs of select MW companions from Weisz et al. (2014). Their properties are listed in Table 2. Left middle: the SFHs of And II and And XVI, plotted identically. Right middle: the SFH of And XVI with comparable luminosity MW companions over-plotted. Right: the SFH of And II with comparable luminosity MW companions over-plotted. Uncertainties have been omitted from the last two panels for clarity.

(A color version of this figure is available in the online journal.)

that took them to their present day locations. Interactions with massive hosts can transform gas-rich dwarf irregulars into gas-poor dwarf spheroidals in a few Gyr via "tidal stirring" (Mayer et al. 2001).

There is some evidence that other M31 satellites were quenched at intermediate epochs similar to And II and And XVI. Shallow CMDs of several other M31 satellites hint at extended SFHs that may have truncated several Gyr ago (e.g., And I, And III, And XII; Da Costa et al. 1996, 2000, 2002; Yang & Sarajedini 2012; Weisz et al. 2014). However, the deepest existing CMDs only extend to the HB, prohibiting any statistically secure claims about quenching timescales; deeper photometry of more systems is needed to explore this scenario.

Intriguingly, well-constrained SFHs from deep CMDs of the M31 halo and outer disk also show strong declines ∼4–6 Gyr ago (Brown et al. 2006; Richardson et al. 2009; Bernard et al. 2012). Speculatively, the coincidental timing may be indicative of a global quenching event in the M31 sub-group perhaps due to a major merger in M31 at intermediate ages (e.g., Fardal et al. 2008; Hammer et al. 2010). However, the detailed evolutionary relationship between a massive host and its satellites is not well understood theoretically or empirically.

5. A COMPARISON WITH THE MW SATELLITES

To facilitate a comparison between the MW and M31 satellite SFHs, we have plotted the cumulative SFHs of 10 MW companions (from Weisz et al. 2014) and our two M31 satellites in Figure 4. We have selected the MW satellites that most resemble our two M31 galaxies in luminosity and current distance from their host galaxy. Their properties are listed in Table 2.

Superficially, it appears that the MW companions and two M31 satellites may simply lie in a continuum of dSphs SFHs, with no regard to host galaxy properties. And II and And XVI both have some balance of ancient and intermediate age populations like most MW companions.

However, there are hints of important differences in this SFH comparison. Most significant is the similarity in the SFHs of And II and And XVI, despite being two orders of magnitude apart in mass. This is in stark contrast to similar pairings of the faint and luminous MW companions which do not show this same degree of similarity in SFHs, e.g., consider the SFHs of Hercules and Leo I. The uniformity in the SFHs of And II and And XVI and absence of similar pairs among the MW companions hints at the potential for unusual evolutionary

Table 2
Global Properties of Select M31 and MW Satellites

Galaxy	M_V	$M_\star$ ($10^6\ M_\odot$)	Distance from Host (kpc)
And II	−12.0	5.3	184
And XVI	−7.5	0.08	279
Hercules	−6.6	0.04	126
CVn I	−8.6	0.23	218
Ursa Minor	−8.8	0.28	78
Draco	−8.8	0.28	76
Carina	−9.1	0.36	107
Leo II	−9.8	0.70	236
Sculptor	−11.1	2.3	86
Leo I	−12.0	5.3	258
Fornax	−13.4	19.0	149

Notes. Luminosities and distances from nearest host for And II, And XVI, and select MW companions. All values from McConnachie (2012), except the luminosities (and stellar masses) of And II and And XVI, which are from N. F. Martin (in preparation). Computation of the stellar masses assume $M_\odot/L_\odot = 1$ and a solar absolute V-band magnitude of 4.80.

behavior in the M31 group. This hypothesis can be further investigated with a larger sample of secure M31 satellite SFHs.

There are also some subtle differences when comparing individual galaxy SFHs. And II is similar in luminosity to MW companions such as Fornax and Leo I. However, its SFH is significantly different. While Fornax and Leo I both show constant SFHs until they were quenched ∼1 Gyr ago ($z \sim 0.1$), And II exhibits a qualitatively different SFH, before it was quenched 5 Gyr ago ($z \sim 0.5$). Sculptor is the next closest in luminosity, but it also exhibits a SFH different from that of And II. In terms of SFH, And II bears some resemblance to Leo II, which also was quenched around a similar time. However, Leo II had a dramatic burst of star formation ∼7 Gyr ago ($z \sim 0.7$) before abruptly being quenched, while And II formed stars steadily over intermediate ages. As it stands, there appears to be no clear analog to And II among the MW satellites.

And XVI also does not appear to have a counterpart in the MW subgroup. And XVI lies at the luminosity boundary between the so-called "ultra-faint" and "classical" dwarfs, but does not share a common SFH with members of either group. The closest analogs are Canes Venatici I and Leo II, which are ∼3–10 times more massive and located ∼50–80 kpc closer to the MW than And XVI is to M31. Leo II also had an intermediate age burst

before its quenching epoch, but it essentially experienced a constant SFH prior to the burst, which is different than And XVI.

And XVI is particularly unusual when compared to similarly low-mass MW companions. The closest in mass is Hercules, which formed >90% of its stellar mass >11 Gyr ago (e.g., Brown et al. 2012). Other, fainter MW satellites appear to have similarly old populations (e.g., Weisz et al. 2014). This comparison demonstrates that And XVI is the lowest mass quenched galaxy known that hosts a predominantly intermediate age population. Leo T and Leo P are of similar stellar mass, but have cold gas and recent star-formation, making them qualitatively different than presently quenched satellites.

6. SUMMARY AND CONCLUSIONS

We have presented new *HST*/ACS-based CMDs of And II and And XVI that reach below the oldest MSTO, making them the deepest observations of satellite galaxies outside of the MW companions. From the deep CMDs, we derived their lifetime SFHs (with an age resolution $\lesssim 1$ Gyr) that can be directly compared to SFHs of the MW satellites with minimal systematic effects. And II and And XVI have similarly extended SFHs: both formed $\sim$50%–70% of their stellar mass prior from 12.5–5 Gyr ago ($z \sim$ 5–0.5), and were abruptly quenched $\sim$5 Gyr ago ($z \sim$ 0.5). This is particular striking as the galaxies are two orders of magnitude apart in stellar mass. Among the MW companions, we find that neither And II nor And XVI have clear analogs, and that similar faint-luminous MW satellite pairings do not have such similar SFHs. Aside from chance coincidence, we discuss plausible physical scenarios to explain their similar SFHs including large scatter in the halo–stellar mass relationship and a global event in the M31 sub-group that may have affected the SFHs of multiple satellites. The extended SFH of And XVI strongly rules out quenching due to reionization, and makes it the lowest mass quenched galaxy ($M_\star \sim 10^5\,M_\odot$) known to host a large intermediate age population. While our findings hint at systematic differences between the M31 and MW satellites, similar quality observations of more M31 satellites are needed for further investigation.

Facility: HST (ACS)

REFERENCES

Amorisco, N. C., Evans, N. W., & van de Ven, G. 2014, Natur, 507, 335
Aparicio, A., & Hidalgo, S. L. 2009, AJ, 138, 558
Assmann, P., Fellhauer, M., Wilkinson, M. I., Smith, R., & Blaña, M. 2013, MNRAS, 435, 2391
Astropy Collaboration, Robitaille, T. P., Tollerud, E. J., et al. 2013, A&A, 558, A33
Belokurov, V., Zucker, D. B., Evans, N. W., et al. 2006, ApJL, 642, L137
Bernard, E. J., Ferguson, A. M. N., Barker, M. K., et al. 2012, MNRAS, 420, 2625
Boylan-Kolchin, M., Bullock, J. S., & Kaplinghat, M. 2011, MNRAS, 415, L40
Brasseur, C. M., Martin, N. F., Macciò, A. V., Rix, H.-W., & Kang, X. 2011, ApJ, 743, 179
Brown, T. M., Smith, E., Ferguson, H. C., et al. 2006, ApJ, 652, 323
Brown, T. M., Tumlinson, J., Geha, M., et al. 2012, ApJL, 753, L21
Busha, M. T., Alvarez, M. A., Wechsler, R. H., Abel, T., & Strigari, L. E. 2010, ApJ, 710, 408
Collins, M. L. M., Chapman, S. C., Rich, R. M., et al. 2014, ApJ, 783, 7
Conn, A. R., Ibata, R. A., Lewis, G. F., et al. 2012, ApJ, 758, 11
Da Costa, G. S., Armandroff, T. E., & Caldwell, N. 2002, AJ, 124, 332
Da Costa, G. S., Armandroff, T. E., Caldwell, N., & Seitzer, P. 1996, AJ, 112, 2576
Da Costa, G. S., Armandroff, T. E., Caldwell, N., & Seitzer, P. 2000, AJ, 119, 705
de Jong, J. T. A., Yanny, B., Rix, H.-W., et al. 2010, ApJ, 714, 663
del Pino, A., Hidalgo, S. L., Aparicio, A., et al. 2013, MNRAS, 433, 1505
Dolphin, A. E. 2000, PASP, 112, 1383
Dolphin, A. E. 2002, MNRAS, 332, 91
Dolphin, A. E. 2012, ApJ, 751, 60
Dolphin, A. E. 2013, ApJ, 775, 76
Fardal, M. A., Babul, A., Guhathakurta, P., Gilbert, K. M., & Dodge, C. 2008, ApJL, 682, L33
Ford, H. C., Bartko, F., Bely, P. Y., et al. 1998, Proc. SPIE, 3356, 234
Gallart, C., Zoccali, M., & Aparicio, A. 2005, ARA&A, 43, 387
Garrison-Kimmel, S., Boylan-Kolchin, M., Bullock, J. S., & Kirby, E. N. 2014, arXiv:1404.5313
Girardi, L., Bertelli, G., Bressan, A., et al. 2002, A&A, 391, 195
Girardi, L., Williams, B. F., Gilbert, K. M., et al. 2010, ApJ, 724, 1030
Hammer, F., Yang, Y. B., Wang, J. L., et al. 2010, ApJ, 725, 542
Hidalgo, S. L., Aparicio, A., Skillman, E., et al. 2011, ApJ, 730, 14
Ho, N., Geha, M., Munoz, R. R., et al. 2012, ApJ, 758, 124
Hunter, J. D. 2007, CSE, 9, 90
Huxor, A. P., Ferguson, A. M. N., Tanvir, N. R., et al. 2011, MNRAS, 414, 770
Ibata, R. A., Lewis, G. F., Conn, A. R., et al. 2013, Natur, 493, 62
Kalirai, J. S., Beaton, R. L., Geha, M. C., et al. 2010, ApJ, 711, 671
Kazantzidis, S., Łokas, E. L., & Mayer, L. 2013, ApJL, 764, L29
Kimble, R. A., MacKenty, J. W., O'Connell, R. W., & Townsend, J. A. 2008, Proc. SPIE, 7010, 70101E
Kirby, E. N., Lanfranchi, G. A., Simon, J. D., Cohen, J. G., & Guhathakurta, P. 2011, ApJ, 727, 78
Lynden-Bell, D. 1976, MNRAS, 174, 695
Martin, N. F., Ibata, R. A., McConnachie, A. W., et al. 2013, ApJ, 776, 80
Mayer, L., Governato, F., Colpi, M., et al. 2001, ApJ, 559, 754
McConnachie, A. W. 2012, AJ, 144, 4
McConnachie, A. W., Arimoto, N., & Irwin, M. 2007, MNRAS, 379, 379
McConnachie, A. W., & Irwin, M. J. 2006, MNRAS, 365, 1263
McConnachie, A. W., Irwin, M. J., Ibata, R. A., et al. 2009, Natur, 461, 66
Monelli, M., Hidalgo, S. L., Stetson, P. B., et al. 2010, ApJ, 720, 1225
Muñoz, J. A., Madau, P., Loeb, A., & Diemand, J. 2009, MNRAS, 400, 1593
Okamoto, S., Arimoto, N., Yamada, Y., & Onodera, M. 2012, ApJ, 744, 96
Oliphant, T. E. 2007, CSE, 9, 10
Pawlowski, M. S., Pflamm-Altenburg, J., & Kroupa, P. 2012, MNRAS, 423, 1109
Pérez, F., & Granger, B. E. 2007, CSE, 9, 21
Pietrinferni, A., Cassisi, S., Salaris, M., & Castelli, F. 2004, ApJ, 612, 168
Planck Collaboration. 2013, arXiv:1303.5076
Richardson, J. C., Ferguson, A. M. N., Mackey, A. D., et al. 2009, MNRAS, 396, 1842
Ricotti, M., & Gnedin, N. Y. 2005, ApJ, 629, 259
Rocha, M., Peter, A. H. G., & Bullock, J. 2012, MNRAS, 425, 231
Sand, D. J., Seth, A., Olszewski, E. W., et al. 2010, ApJ, 718, 530
Schlafly, E. F., & Finkbeiner, D. P. 2011, ApJ, 737, 103
Shaya, E. J., & Tully, R. B. 2013, MNRAS, 436, 2096
Sohn, S. T., Besla, G., van der Marel, R. P., et al. 2013, ApJ, 768, 139
Starkenburg, E., Helmi, A., De Lucia, G., et al. 2013, MNRAS, 429, 725
Stetson, P. B. 1994, PASP, 106, 250
Tollerud, E. J., Beaton, R. L., Geha, M. C., et al. 2012, ApJ, 752, 45
Tolstoy, E., Hill, V., & Tosi, M. 2009, ARA&A, 47, 371
Tolstoy, E., Irwin, M. J., Helmi, A., et al. 2004, ApJL, 617, L119
Weisz, D. R., Dolphin, A. E., Skillman, E. D., et al. 2014, arXiv:1404.7144
Yang, S.-C., & Sarajedini, A. 2012, MNRAS, 419, 1362